BTK modulates p53 activity to enhance apoptotic and senescent responses

Mohammad Althubiti[a,b], Miran Rada[a,b], Jesvin Samuel[a,b], Josep M. Escorsa[a,b], Hishyar Najeeb[b,c], Koon-Guan Lee[d], Kong-Peng Lam[d], George D. D. Jones[b,c], Nickolai Barlev[e], and Salvador Macip[a,b]*

[a]Mechanisms of Cancer and Aging Laboratory, Department of Molecular and Cell Biology, University of Leicester, Leicester, UK. [b]Cancer Research UK Leicester Centre. [c]Department of Cancer Studies, University of Leicester, Leicester, UK. [d]Bioprocessing Technology Institute, A*STAR, Singapore. [e]Institute of Cytology, RAS, Saint-Petersburg, Russia.

*Corresponding author: Salvador Macip. Department of Molecular and Cell Biology, University of Leicester, University Road, Leicester, LE1 7RH, UK. sm460@le.ac.uk, Phone: +44 (0)116 229 7113. Fax: +44 (0)116 229 7123.

Running title: Role of BTK in the p53 pathway.

ABSTRACT

p53 is a tumor suppressor that prevents the emergence of transformed cells by inducing apoptosis or senescence, among other responses. Its functions are tightly regulated by post-translational modifications. Here, we show that Bruton's Tyrosine Kinase (BTK) is a novel modulator of p53. We found that BTK is induced in response to DNA damage and p53 activation. This leads to the phosphorylation of p53, which constitutes a positive feedback loop that increases p53 protein levels and enhances the transactivation of its target genes in response to stress. Inhibiting BTK reduced both p53-dependent senescence and apoptosis. Moreover, BTK expression also induced up-regulation of DNA damage signals and apoptosis. We conclude that, despite being involved in oncogenic signals in blood malignancies, BTK has antineoplastic properties in other contexts, such as the enhancement of p53 tumor suppressor responses. This is supported by the fact that BTK expression correlates with good prognosis in some epithelial tumors. The clinical use of BTK inhibitors should be evaluated in the light of these findings.

INTRODUCTION

The tumor suppressor p53 mediates cellular responses to DNA damage (1). It is a transcription factor that prevents the transformation of cells by triggering protective mechanisms such as cell cycle arrest or apoptosis (2, 3). Several factors cooperate to determine cell fates induced by p53 after stress, although not all of them are known (4). p53 is regulated post-translationally through many different modifications, including phosphorylation, methylation and acetylation (3, 5-8). Its N-terminal region has an important role in its stability, since the E3 ligase MDM2 binds to it and ubiquitinates p53, which is then targeted for proteasomal degradation (9). Different stresses lead to phosphorylation of residues in the N-terminal region, including serine 15, which disrupts the MDM2-p53 interaction and thus increases the half-life of p53 (10, 11).

An important cellular response to p53 is senescence, a permanent cell cycle arrest with specific morphological features in which cells remain metabolically active (12). The establishment of this phenotype may be a response to stress (stress-induced premature senescence) or telomere shortening after a number of cell divisions (replicative senescence) (13). Senescent cells are present in pre-malignant and early stages of solid cancers, after which they disappear, which suggests that the senescent barrier needs to be overcome in order to progress into malignancy (14). Senescence has also been associated with age-dependent organismal changes, and the accumulation of senescent cells with time has been shown to contribute to the functional organ impairment seen in aging (15).

BTK is a non-receptor tyrosine kinase mutated in the inherited immunodeficiency disease X-linked agammaglobulinemia (16). It is expressed in myeloid and lymphoid cells but not in T cells and it is a member of the Tec family of kinases, which play a role in B-cell receptor (BCR)

signaling (17). In B cells, BTK is activated after an antigen binds to the BCR, which leads to its phosphorylation at tyrosine 551 by SRC family kinases and its autophosphorylation at tyrosine 223 (18). Although BTK is mainly located at the cell membrane, it can also be found in the nucleus (19). A pathological BTK up-regulation has been shown in B cell malignancies such as chronic lymphocytic leukemia (CLL), Mantle cell lymphoma, and multiple myeloma (20-22). Small molecule inhibitors of BTK have been developed to treat these diseases. Ibrutinib (PCI-32765), which irreversibly binds to C481 and inhibits Y223 stimulation (23), has been approved to treat mantle lymphoma and CLL (24). Another BTK inhibitor, CGI-1746, reversibly binds to the SH3 domain and blocks phosphorylation at Y551, thus keeping the protein in its inactive form (25).

We found that BTK was induced in a screening of markers for senescent cells (26). Exploring this, here we show that BTK is involved in the p53 pathway as a modulator of its activity. We propose that, in opposition to its oncogenic role in B cells, BTK can be expressed in response to damage and contributes to the tumor suppressor mechanisms regulated by p53.

MATERIALS AND METHODS

Cell Culture and chemicals. Human diploid dermal fibroblasts (HDF), HCT116 and HT1080 were maintained in DMEM supplemented with 10% fetal bovin serum (Gibco) and penicillin-streptomycin (50U/ml). EJp53 were maintained as described (27). EJp53 were a gift from Dr. S. Aaronson (Mount Sinai School of Medicine, New York, 2008), HCT116 from Dr. B. Vogelstein (Johns Hopkins University, Baltimore, 2008) and HT1080 from Dr I. Roninson (South Carolina

College of Pharmacy, Charleston, 2008). HDF were obtained from ATCC (2014). All cells were expanded and stored in liquid nitrogen when received and original vials were thawed for these experiments. No further validation or authentication was performed. Chemicals: Ibrutinib (Sellechem, PCI-32765), CGI-1746 (Axon Medchem, 2018), Tert-Butylhydroperoxide (Merck), doxorubicin (Sigma-Aldrich), sotrastaurin (Sellechem) and dactolisib (Sellechem). Peripheral blood samples were obtained from patients with Chronic Lymphocytic Leukaemia (CLL) after informed consent and approval from the Local Research Ethics Committee. The patients were treatment naïve and had a cell count >50 x 10^9/l. Peripheral blood mononuclear cells (PBMCs) were processed as previously described (28). An adenovirus containing p53 (Adp53), a gift of B. Vogelstein (Johns Hopkins University, Baltimore), or LacZ (AdLacZ) were amplified as previously described (29). Cells were exposed to 10 µl of the appropriately diluted virus stock.

PPISURV analysis. PPISURV (30) was used to correlate survival rates in cancer patients to the expression level of BTK. In each data set, samples were grouped with respect to expression rank of the gene, which reflects relative mRNA expression level and introduces no normalization bias. The 'low expression' and 'high expression' groups are those where expression rank of the gene is less or more than average expression rank across the data set, respectively. This separation of patients into 'low' and 'high' groups in the data set along with survival information is next used to find statistical differences in survival outcome. The R statistical package was used to perform survival analyses and to draw KM plots. Unadjusted P-values were generated using standard survival analysis packages.

Growth curves. 1×10^4 cells were plated in 6 cm plates a day before chemicals were added. Cells were counted every 4 days using a BIO-RAD TC20 automated cell counter, after which fresh media and chemicals were added to the cultures.

Immunoblot Analysis. Western blots were performed as described (31). Primary antibodies used: anti-phospho-Histone 2A (ser 139, Millipore 05-636), anti-phosphoATM (S1918, Abcam ab81292), anti-phospho-p53 (ser 15, Cell Signalling 9284), anti-p53 (DO-1, Santa Cruz, sc-129), anti-BTK (D3H, Cell Signalling 8547), anti-p16 (abcam ab54210), anti-β-actin (Abcam ab8227) and anti-caspase 3 (Cell Signalling 96625), anti-PARP-1 (Cell Signalling 9542). An ECL detection system (Thermo Scientific) was used to visualize the results. Alternatively, an Odyssey CLx Infrared Imaging System (Li-COR) was used. For Ponceau staining, 1x Ponceau staining (Sigma, P 3504) was added to the membrane for 5 min with shaking.

Immunofluorescence. Cells were processed as previously described (26). Coverslips were incubated overnight at 4°C with 1: 50 anti-BTK (D3H5, Cell Signalling 8547) or 1:100 anti-p53-FITC (Santa Cruz sc-126). Secondary anti-rabbit (1:500) antibody (Alexa Fluor 594, Invitrogen) and DAPI (Invitrogen) were used. Slides were analyzed using a Nikon TE300 microscope.

Senescence-associated-β-Galactosidase (SA-β-Gal) staining. Cells were stained as previously described (32)**.**

Colony formation assay. 500 cells were split into 60 mm plates in triplicates and assays were performed as described (31).

BTK Overexpression. Transfection was performed using Lipofectamine 2000 (Invitrogen) following manufacturer's protocols. 8μg of empty plasmid (Mission pLKO.1 Empty vector control plasmid DNA, Sigma Aldrich SHC001) or a BTK plasmid (OriGene RG211582) were used. Medium was changed after 5 hours and cells were left for 18-24 hours.

BTK Silencing. shRNA against BTK (Santa Cruz sc-29841-sh) or luciferase (control, Sigma Aldrich SHC007, Mission pLKO.1puro Luciferase) were transfected into EJp53 and HCT116 using Lipofectamine 2000 following manufacturer's protocols using 1μg of shRNA. 2 μg/ml puromycin was added for 2 weeks to select for transfected cells.

Quantitative real time PCR. RNA purification, cDNA preparation and qRT-PCR were performed as previously described (33). Primers used: PUMA: GACCTCAACGCACAGTACGA (FWD), CACCTAATTGGGCTCCATCT (REV). p21: CACCGAGACACCACTGGAGG (FWD), GAGAAGATCAGCCGGCGTTT (REV). GAPDH: GGGAAGGTGAAGGTCGGAGT (FWD), TTGAGGTCAATGAAGGGGTCA (REV). BTK: ACAGATTCCGAGGAGAGGTGAGG (FWD), GGTCCTTCATCATATACAACCTGGAATGG (REV).

ChIP Assays. ChIP assays were performed as previously described (34). 3×10^6 cells per sample were used. PCR was performed with 1 μl of DNA. The p53 (Ab-6, Galbichem#OP43) antibody was used. Primers used: PUMA, GCGAGACTGTGGCCTTGTGT (FWD), CGTTCCAGGGTCCACAAAGT (REV); p21, GTGGCTCTGATTGGCTTTCTG (FWD),

7

CTGAAAACAGGCAGCCCAAG (REV); Actin, TGGCTCAGCTTTTTGGATTC (FWD), CCGAGGATTGGAGAAGCAGT (REV).

Luciferase Reporter Assay. 100,000 cells per well were seeded in 0.5ml growth media in 24-well plates the day before transfection. Transfection was performed with Turbofect (Life Technologies #R0531) using manufacturer's protocol. 1.0μg total plasmid DNA (0.3 μg luciferase construct, 0.2 μg β-galactosidase construct, and 0.5μg empty control vector or BTK construct) was used. 24 hours after transfection, media was replaced by fresh growth media and part of samples was treated with 1.0μM Doxorubicin. 20 hours later, lysates were collected in lysis buffer and stored at -80°C overnight. (10ml of β-galactosidase stock solution, 20 mg o-nitrophenyl-β-d-galactopyranoside (ONPG) and 35μl β-mercaptoethanol and 100 μl β-galactosidase substrate were added to 80μl cell lysate (per well) in a 96-well transparent plate. This was incubated at 37°C for 15 minutes. 20μl of the cell lysate were transferred to a 96-well opaque white plate and read in a luminometer, using a luciferase kit (BioVision#K801-200), following manufacturer's instructions. Luminescence was measured at a wavelength of 450 nm with a luminometer spectrometer (PerkinElmer VICTOR X). Relative luciferase activity was calculated by first dividing the luminescence value of each sample by its B-gal value and then presenting the result as a fold difference between each sample and the control sample.

In vitro **kinase activity assay.** Full length of Recombinant BTK (Invitrogen,PV3363) and different regions p53 of were used in this study. The GST-tagged fragments of p53 were obtained by transfecting the appropriate pGEX vectors into BL21 competent and purifying the proteins produced with glutathione HiCap matrix beads (Qiagen #30900), as previously

described (6). To examine the ability of BTK to phosphorylate p53, 0.5 µg of BTK and 0.5 µg of different GST-p53 proteins were added in tube contained 25 µl of the kinase buffer (12.5 mM (pH7.5), 10 mM MgCl$_2$, 1 mM EGTA, 0.5 mM Na$_3$ VO$_4$, 5 mM β-Glycerophosphate, 0.01% Triton X-100, 2 mM DTT, 200 µM ATP). Approximately, 0.37 MBq of [^{32}P] γ-ATP was added to each tube for 30 min at 30 ^{0}C. Loading buffer was then added to each sample, and samples were boiled for 5 min and loaded into 10% polyacrylamide gel. The gel was then dried using a Model v583 Gel drier (Biorad) for 1 hour and exposed to film in a Phosphor screen (GH Healthcare) overnight at room temperature. Phospho-image of dried gel was then developed using a Typhoon TRIO+ Variable mode manger scanner (GE Healthcare).

Comet assay. 40,000 cells were processed as described (35). Briefly, 170 µl of 0.6% low melting point agarose was added to the cell pellet. 80 µl of the mixture was placed onto the pre-coated slides with normal melting point agarose and covered by a coverslip. After the gel became solid, cover slips were removed and slides kept in lysis buffer (2.5 M NaCl, 0.1 M Na$_2$EDTA, 10 mM Tris-HCl, 1% TritonX-100 at pH 10) overnight. Slides were then washed for 20 minutes with ice cold ddH$_2$O, protected from light, and exposed to ice cold alkaline buffer (pH >13) for 20 minutes, protected from light. This step allows the unwinding of the DNA before applying the current at 30v/300mA for further 20 minutes. Slides were washed twice for 5 minutes with ddH$_2$O, and placed at 37º C overnight. Slides were rehydrated with ice cold ddH$_2$O for 30 minutes at room temperature and stained with Propidium iodide (2.5 5µg/ml) for further 20 minutes, then washed with fresh ddH$_2$O for 20 minutes and placed in an oven before being scored with a fluorescence microscope. Comets were visualized in the fluorescence microscope at a magnification of 200×. Images were captured and analyzed with the Komet Analysis

software version 5.5 (Andor Bioimaging, Nottingham, UK). 100 cells were analyzed per sample, 50 per duplicate slide. The percentage of DNA in the tail of the comet was calculated for each cell by the software.

Statistical analysis. All error bars represent the standard deviation. Statistical significance (not significant, ns: $P > 0.05$; *: $P \leq 0.05$; ** $P \leq 0.01$; ***: $P \leq 0.001$; ****: $P \leq 0.0001$) was calculated using two-tailed unpaired t-tests with Prism 6 (GraphPad) software.

RESULTS

BTK is induced in p53-mediated DNA damage responses. In a proteomics screen (26), we identified Bruton's tyrosine kinase (BTK) as a protein induced in cells undergoing senescence. BTK, a non-receptor kinase involved in BCR signaling (16), is highly expressed in different types of leukemia and lymphomas (36) and this has led to BTK inhibitors being used to treat B-cell malignancies (25). To better understand the role of BTK in tumor suppressor pathways, we used EJp53, a p53-null bladder cancer cell line with a tetracycline (tet)-regulatable p53 expression system (27). We found that BTK protein levels were elevated after inducing p53 expression in these cells (Figure 1A). Moreover, the colon cancer cell line HCT116, which has wild type p53, also showed a p53-dependent BTK induction after being treated with DNA damaging agents (the oxidant tBH and doxorubicin), both at protein (Figures 1B and C) and mRNA levels (Figure 1D). This suggests a direct correlation between the induction of p53 and BTK. Using PPISURV (30), we analyzed survival rates in cancer patients and found that, despite high expression of BTK correlating with a poor prognostic in CLL, as expected (25, 36), it was a

10

marker of good prognosis in breast and lung cancer (Figure 1E). These data together suggest the involvement of BTK in p53-mediated responses to cellular damage and tumor suppression.

BTK increases p53 protein levels and its phosphorylation. We next investigated the details of the contribution of BTK to the p53 pathway. We transfected BTK into EJp53 and observed that it elevated the levels of p53 protein induced by tet removal (Figure 2A). This was also evident in HCT116, in which BTK expression increased p53 levels in the presence or absence of DNA damaging agents (Figure S1A). Of note, BTK expression was not sufficient to induce nuclear localization of p53 (Figure S1A), which was otherwise evident after damage. Moreover, it did not increase the levels of p53 mRNA (Figure 2B), which indicated a potential involvement of BTK in the post-transcriptional modifications of p53. To test this possibility, we used Ibrutinib, a BTK inhibitor recently approved to treat different forms of leukemia (23), CGI-1746, a more specific BTK inhibitor (25), and an EJp53 stably expressing a shRNA against BTK (Figure S1B). Blocking BTK by any of these methods severely reduced the levels of p53 induced by tet removal in EJp53, both after short and long term inhibition (Figures 2C and D). Reduction in p53 protein levels in the absence of BTK was also observed in EJp53 and HCT116 infected with an adenovirus containing p53 (Figure S1C), as well as primary malignant B cells stimulated with CD154 and IL4, a culture protocol that we observed induces p53 expression (Figure S1D). This shows that the effects of BTK on p53 levels can be seen in different models of p53 induction and confirms that BTK is involved in the stabilization of p53 protein levels.

We reasoned that the positive effects of BTK on p53 accumulation could be mediated by phosphorylation, the most common mechanism of p53 regulation (5). AS shown in Figure 2E, we found that BTK was able to phosphorylate p53 *in vitro* and, using recombinant peptides

11

(Figure S2A), we predicted that this phosphorylation takes place mainly in residues 1 to 80 of p53. This region of p53 contains serine 15 (S15), which is important in the MDM2-mediated regulation of p53 protein levels (5). Using a phospho-specific antibody, we confirmed that BTK increases S15 phosphorylation in cells in the presence or absence of DNA damage (Figure 2F). Moreover, a S15A p53 mutant showed reduced phosphorylation by BTK *in vitro* (Figure S2B). p53 is known to be phosphorylated by ATM, ATR, DNA-PK and PKC (37), among other kinases. Using specific inhibitors, such as dactolisib (38) and sotrastaurin (39), we found that the effects of BTK on p53 activity were independent of all these kinases (Figure S2C), suggesting a direct phosphorylation. This data together indicates that BTK increases the phosphorylation of p53 at S15, among other residues at the N terminus, which would result in the disruption of MDM2-p53 interactions and thus provide a mechanism for the increase in p53 stability.

BTK enhances the transactivation of p53 target genes. Our data shows that BTK is important for the phosphorylation and stabilization of p53. This suggests that it could play a role in enhancing p53 activity**.** We explored this hypothesis by measuring the effect of BTK on the expression of p53 target genes. As shown in Figure 3A, BTK increased the up-regulation of the mRNA of both p21 and PUMA after treatment with doxorubicin. This was confirmed by a higher activity of the luciferase reporters in the presence of BTK (Figure 3B). Finally, a ChIP analysis showed increased binding of p53 to the p21 and PUMA promoters after DNA damage when BTK was expressed (Figure 3C). In these experiments, BTK did not significantly increase the activity of p53 in the absence of damage, which is consistent with the fact that although p53 can be induced by BTK expression alone, it remains in the cytosol and it is thus inactive (see Figure S1A). Importantly, when a BTK lacking the kinase domain (40) was expressed, the increase in

luciferase activity of the p21 reporter was not observed (Figures 3D and E), indicating that the positive effects on p53 transactivation are mediated by the kinase activity of BTK.

BTK inhibition blocks p53-induced senescence. We next studied the involvement of BTK in the cellular responses to p53. As shown in Figure 4A, inhibition of BTK by chemical or genetic approaches increased cell proliferation in EJp53 induced to senesce. The inhibition of the permanent growth arrest was confirmed by the fact that the morphological changes associated with senescence were not as evident in cells in which BTK had been blocked (Figure 4B) and that these cells were able to form colonies (Figure 4C). EJp53 are a representative model of stress-induced premature senescence (41). To expand our observations, we also investigated whether BTK plays a role in replicative-induced senescence by serially passaging normal human fibroblasts in the presence of BTK inhibitors. As shown in Figure 4D, Ibrutinib was able to delay the growth arrest of fibroblasts as they entered senescence. Moreover, expression of p16 (a well-known marker of senescence (42)) was reduced in late passage cells when BTK was inhibited, similarly to what happened to the levels of p53 (Figure 4E). This suggests that replicative senescence was also delayed in the absence of BTK. Indeed, the percentage of cells positive for Senescence Associated (SA)-β-gal, a widely used marker of senescence (32), was significantly lower when BTK was inhibited, and less cells showed the morphological changes typical of senescence (Figure 4F). Collectively, these results indicate that BTK has a critical role in inducing and/or maintaining both p53-dependent stress-induced and replicative senescence.

BTK expression induces DNA damage signals and apoptotic responses. Our results suggest a new role for BTK in tumor suppressor responses in epithelial cells. We further explored this by

13

studying the role of BTK in DNA damage responses. We first transfected BTK into HCT116 (Figure 5A) and measured the activation of elements of the DNA damage pathways. We found that BTK expression leads to the phosphorylation of ATM and H2AX (Figure 5B). BTK induced ATM in normal fibroblasts as well (Figure S3A). This correlated with increased damage to DNA, as measured by a comet assay (Figure 5C). Together with this, we observed that BTK expression was able to induce apoptosis in HCT116 cells, as measured by PI and Annexin V stainings (Figure 5D) as well as cleavage of caspase 3 and PARP (Figure 5E). Moreover, this was also observed in EJp53 cells in the absence of p53 expression (Figure S3B), which suggests that it is at least in part p53-independent. BTK prevented EJp53 growth (Figure S3C) and colony formation (Figure S3D), similarly to the expression of p53. Finally, inhibition of BTK by Ibrutinib in HCT116 cells treated with doxorubicin significantly reduced the amount of cell death induced by the drug (Figure 5F), thus confirming the involvement of BTK in the response to DNA damage in these cells. These data together suggest a pro-apoptotic and anti-proliferative role of BTK that relies on its participation in DNA damage pathways and may not depend completely on its effects on p53.

DISCUSSION

Our study reveals that BTK is a novel modulator of p53 activity and is involved in the cellular response to DNA damage. Although BTK has been implicated in oncogenic signaling in blood malignancies (16), here we show that it can also participate in tumor suppressor pathways. This is consistent with previous reports that also uncovered pro-apoptotic and antineoplastic

14

properties of BTK (43, 44) (45). This suggests that BTK expression has radically different functions depending on the cellular context, which would include being part of pro-survival pathways in B cells and enhancing arrest/death signals in damaged epithelial cells. This paradox is supported by our bioinformatics analysis, which shows an opposed prognostic value of BTK levels of expression in blood malignancies and solid tumors (see Figure 1E).

Our experiments also allowed us to propose a mechanism by which BTK impacts on cell fate responses to damage. We found that following BTK expression, there is an increase in p53 phosphorylation at S15, among other residues, which would explain the BTK-mediated stabilization of p53 protein levels (5). This is independent of the activity of the kinases that most commonly phosphorylate p53 in response to damage, such as ATM, ATR, DNA-PK or PKC. Although it would have to be further confirmed, this suggests that BTK could be directly phosphorylating p53 to activate it. Of note, despite being originally described as a tyrosine kinase, BTK is known to be able to phosphorylate serines as well (46), which would fit this hypothesis. Nevertheless, we found that BTK can increase ATM and γH2AX, consistent with a role in enhancing of DNA damage signals.

We also confirmed that the kinase function of BTK is essential for its effects on p53 accumulation. However, p53 still needs to be activated by other signals in the DNA damage pathway in order to relocate to the nucleus. All our data indicate that BTK is not sufficient to activate p53 on its own, but that it can increase its activity in the context of a DNA damage response. Indeed, we have observed that BTK expression increases the binding of p53 to the promoters of its target genes after genotoxic stress, which results in higher levels of expression of both pro-apoptotic and pro-arrest signals.

The importance of BTK in the different cellular responses to p53 is underscored by the consequences of its inhibition, since using both chemical inhibitors and RNAi we showed that p53 accumulation is compromised. The potential neoplastic effects of inhibiting BTK in clinical settings should need to be carefully considered. Large cohorts of patients are currently being given BTK inhibitors for the treatment of leukemia, which our results suggest could potentially affect p53 activity. So far there have been no reports of increased incidence of secondary malignancies but our data suggests that it is a possibility that should be studied.

Inhibition of BTK results in the partial blocking of p53-induced senescence, which shows that BTK is a novel regulator of this tumor suppressor pathway. This is especially relevant because, despite the considerable knowledge accumulated in the fifty years since Leonard Hayflick first described cellular senescence (47), the molecular pathways involved in this phenotype are still incompletely characterized. Our results show that in the absence of BTK, p53-dependent senescence can be partially avoided and cells are allowed to continue growing, probably as a direct consequence of p53 protein levels being strongly reduced. Moreover, replicative senescence, which also relies on other triggers, such as p16 (42), was also delayed in the absence of BTK, which suggests that BTK could also be contributing to this phenotype in a p53-independent manner. These results provide a rationale to use BTK inhibitors to block senescence in those situations in which it has a negative effect on the organism. For instance, they could have a therapeutic effect on diseases in which senescent cell accumulation is thought to be important, such as diabetes, osteoporosis, COPD or neurodegenerative disorders (48). The accumulation of senescent cells strongly contributes to the progression of breast cancers (49) and this could also be avoided with the adequate regime of BTK inhibitors.

We observed that blocking BTK reduces p53-induced apoptosis as well. We show that BTK can have pro-apoptotic effects when overexpressed, which suggests that it could contribute to apoptotic signals in certain contexts, even in the absence of p53. Since we have shown that DNA damage signals are activated when BTK is expressed, it would be important to characterize other effects of BTK in these pathways, directly or through indirect mechanisms. We propose that the role of BTK on enhancing p53-dependent cell death is likely to be at least at two different levels: it would be important to stabilize p53 through phosphorylation and it would also contribute apoptotic signals independently.

In summary, our data presents a new side of BTK as a key modulator of p53 functions, being involved in a positive feedback loop that links its induction after p53 up-regulation to its stabilization of p53. Thus, BTK emerges as a pro-apoptotic kinase and an important regulator of p53-mediated senescence and apoptosis. This underscores the complexity of BTK functions, which can sometimes be antagonistic and are likely to be determined by cellular context.

REFERENCES

1.   Lane DP. Cancer. p53, guardian of the genome. Nature. 1992;358:15-6.

2.   Vousden KH, Lane DP. p53 in health and disease. Nature reviews Molecular cell biology. 2007;8:275-83.

3.   Marouco D, Garabadgiu AV, Melino G, Barlev NA. Lysine-specific modifications of p53: a matter of life and death? Oncotarget. 2013;4:1556-71.

4.   Murray-Zmijewski F, Slee EA, Lu X. A complex barcode underlies the heterogeneous response of p53 to stress. Nature reviews Molecular cell biology. 2008;9:702-12.

5.   Dai C, Gu W. p53 post-translational modification: deregulated in tumorigenesis. Trends in molecular medicine. 2010;16:528-36.

6.   Barlev NA, Liu L, Chehab NH, Mansfield K, Harris KG, Halazonetis TD, et al. Acetylation of p53 activates transcription through recruitment of coactivators/histone acetyltransferases. Molecular cell. 2001;8:1243-54.

7.   Chuikov S, Kurash JK, Wilson JR, Xiao B, Justin N, Ivanov GS, et al. Regulation of p53 activity through lysine methylation. Nature. 2004;432:353-60.

8.   Ivanov GS, Ivanova T, Kurash J, Ivanov A, Chuikov S, Gizatullin F, et al. Methylation-acetylation interplay activates p53 in response to DNA damage. Molecular and cellular biology. 2007;27:6756-69.

9.   Wade M, Li YC, Wahl GM. MDM2, MDMX and p53 in oncogenesis and cancer therapy. Nature reviews Cancer. 2013;13:83-96.

10.   Durocher D, Jackson SP. DNA-PK, ATM and ATR as sensors of DNA damage: variations on a theme? Curr Opin Cell Biol. 2001;13:225-31.

11.   Jazayeri A, Falck J, Lukas C, Bartek J, Smith GC, Lukas J, et al. ATM- and cell cycle-dependent regulation of ATR in response to DNA double-strand breaks. Nature cell biology. 2006;8:37-45.

12.   Collado M, Serrano M. Senescence in tumours: evidence from mice and humans. Nature reviews Cancer. 2010;10:51-7.

13.   Campisi J, d'Adda di Fagagna F. Cellular senescence: when bad things happen to good cells. Nature reviews Molecular cell biology. 2007;8:729-40.

14.   Collado M, Gil J, Efeyan A, Guerra C, Schuhmacher AJ, Barradas M, et al. Tumour biology: senescence in premalignant tumours. Nature. 2005;436:642.

15. Lopez-Otin C, Blasco MA, Partridge L, Serrano M, Kroemer G. The hallmarks of aging. Cell. 2013;153:1194-217.

16. Vetrie D, Vorechovsky I, Sideras P, Holland J, Davies A, Flinter F, et al. The gene involved in X-linked agammaglobulinaemia is a member of the src family of protein-tyrosine kinases. Nature. 1993;361:226-33.

17. Bradshaw JM. The Src, Syk, and Tec family kinases: distinct types of molecular switches. Cellular signalling. 2010;22:1175-84.

18. Rawlings DJ, Scharenberg AM, Park H, Wahl MI, Lin S, Kato RM, et al. Activation of BTK by a phosphorylation mechanism initiated by SRC family kinases. Science. 1996;271:822-5.

19. Gustafsson MO, Hussain A, Mohammad DK, Mohamed AJ, Nguyen V, Metalnikov P, et al. Regulation of nucleocytoplasmic shuttling of Bruton's tyrosine kinase (Btk) through a novel SH3-dependent interaction with ankyrin repeat domain 54 (ANKRD54). Molecular and cellular biology. 2012;32:2440-53.

20. Herman SE, Gordon AL, Hertlein E, Ramanunni A, Zhang X, Jaglowski S, et al. Bruton tyrosine kinase represents a promising therapeutic target for treatment of chronic lymphocytic leukemia and is effectively targeted by PCI-32765. Blood. 2011;117:6287-96.

21. Chang BY, Francesco M, De Rooij MF, Magadala P, Steggerda SM, Huang MM, et al. Egress of CD19(+)CD5(+) cells into peripheral blood following treatment with the Bruton tyrosine kinase inhibitor ibrutinib in mantle cell lymphoma patients. Blood. 2013;122:2412-24.

22. Kuehl WM, Bergsagel PL. Molecular pathogenesis of multiple myeloma and its premalignant precursor. The Journal of clinical investigation. 2012;122:3456-63.

23.   Honigberg LA, Smith AM, Sirisawad M, Verner E, Loury D, Chang B, et al. The Bruton tyrosine kinase inhibitor PCI-32765 blocks B-cell activation and is efficacious in models of autoimmune disease and B-cell malignancy. Proceedings of the National Academy of Sciences of the United States of America. 2010;107:13075-80.

24.   Aalipour A, Advani RH. Bruton's tyrosine kinase inhibitors and their clinical potential in the treatment of B-cell malignancies: focus on ibrutinib. Therapeutic advances in hematology. 2014;5:121-33.

25.   Di Paolo JA, Huang T, Balazs M, Barbosa J, Barck KH, Bravo BJ, et al. Specific Btk inhibition suppresses B cell- and myeloid cell-mediated arthritis. Nature chemical biology. 2011;7:41-50.

26.   Althubiti M, Lezina L, Carrera S, Jukes-Jones R, Giblett SM, Antonov A, et al. Characterization of novel markers of senescence and their prognostic potential in cancer. Cell death & disease. 2014;5:e1528.

27.   Macip S, Igarashi M, Berggren P, Yu J, Lee SW, Aaronson SA. Influence of induced reactive oxygen species in p53-mediated cell fate decisions. Molecular and cellular biology. 2003;23:8576-85.

28.   Willimott S, Baou M, Naresh K, Wagner SD. CD154 induces a switch in pro-survival Bcl-2 family members in chronic lymphocytic leukaemia. British journal of haematology: Blackwell Publishing Ltd; 2007. p. 721-32.

29.   He TC, Zhou S, da Costa LT, Yu J, Kinzler KW, Vogelstein B. A simplified system for generating recombinant adenoviruses. Proceedings of the National Academy of Sciences of the United States of America. 1998;95:2509-14.

30.   Antonov AV, Krestyaninova M, Knight RA, Rodchenkov I, Melino G, Barlev NA. PPISURV: a novel bioinformatics tool for uncovering the hidden role of specific genes in cancer survival outcome. Oncogene. 2014;33:1621-8.

31.   Carrera S, de Verdier PJ, Khan Z, Zhao B, Mahale A, Bowman KJ, et al. Protection of cells in physiological oxygen tensions against DNA damage-induced apoptosis. The Journal of biological chemistry. 2010;285:13658-65.

32.   Dimri GP, Lee X, Basile G, Acosta M, Scott G, Roskelley C, et al. A biomarker that identifies senescent human cells in culture and in aging skin in vivo. Proceedings of the National Academy of Sciences of the United States of America. 1995;92:9363-7.

33.   Carrera S, Senra J, Acosta MI, Althubiti M, Hammond EM, de Verdier PJ, et al. The Role of the HIF-1alpha Transcription Factor in Increased Cell Division at Physiological Oxygen Tensions. PloS one. 2014;9:e97938.

34.   Lezina L, Purmessur N, Antonov AV, Ivanova T, Karpova E, Krishan K, et al. miR-16 and miR-26a target checkpoint kinases Wee1 and Chk1 in response to p53 activation by genotoxic stress. Cell death & disease. 2013;4:e953.

35.   Carrera S, Cuadrado-Castano S, Samuel J, Jones GD, Villar E, Lee SW, et al. Stra6, a retinoic acid-responsive gene, participates in p53-induced apoptosis after DNA damage. Cell Death Differ. 2013.

36.   Hendriks RW, Yuvaraj S, Kil LP. Targeting Bruton's tyrosine kinase in B cell malignancies. Nature reviews Cancer. 2014;14:219-32.

37.   Lakin ND, Jackson SP. Regulation of p53 in response to DNA damage. Oncogene. 1999;18:7644-55.

38.   Mukherjee B, Tomimatsu N, Amancherla K, Camacho CV, Pichamoorthy N, Burma S. The dual PI3K/mTOR inhibitor NVP-BEZ235 is a potent inhibitor of ATM- and DNA-PKCs-mediated DNA damage responses. Neoplasia. 2012;14:34-43.

39.   Wagner J, von Matt P, Sedrani R, Albert R, Cooke N, Ehrhardt C, et al. Discovery of 3-(1H-indol-3-yl)-4-[2-(4-methylpiperazin-1-yl)quinazolin-4-yl]pyrrole-2,5-dione   (AEB071),   a   potent and selective inhibitor of protein kinase C isotypes. Journal of medicinal chemistry. 2009;52:6193-6.

40.   Lee KG, Kim SS, Kui L, Voon DC, Mauduit M, Bist P, et al. Bruton's tyrosine kinase phosphorylates DDX41 and activates its binding of dsDNA and STING to initiate type 1 interferon response. Cell reports. 2015;10:1055-65.

41.   Sugrue MM, Shin DY, Lee SW, Aaronson SA. Wild-type p53 triggers a rapid senescence program in human tumor cells lacking functional p53. Proceedings of the National Academy of Sciences of the United States of America. 1997;94:9648-53.

42.   Munoz-Espin D, Serrano M. Cellular senescence: from physiology to pathology. Nature reviews Molecular cell biology. 2014;15:482-96.

43.   Middendorp S, Zijlstra AJ, Kersseboom R, Dingjan GM, Jumaa H, Hendriks RW. Tumor suppressor function of Bruton tyrosine kinase is independent of its catalytic activity. Blood. 2005;105:259-65.

44.   Islam TC, Branden LJ, Kohn DB, Islam KB, Smith CI. BTK mediated apoptosis, a possible mechanism for failure to generate high titer retroviral producer clones. The journal of gene medicine. 2000;2:204-9.

45.   Kersseboom R, Middendorp S, Dingjan GM, Dahlenborg K, Reth M, Jumaa H, et al. Bruton's tyrosine kinase cooperates with the B cell linker protein SLP-65 as a tumor suppressor in Pre-B cells. The Journal of experimental medicine. 2003;198:91-8.

46.   Yang EJ, Yoon JH, Chung KC. Bruton's tyrosine kinase phosphorylates cAMP-responsive element-binding protein at serine 133 during neuronal differentiation in immortalized hippocampal progenitor cells. The Journal of biological chemistry. 2004;279:1827-37.

47.   Hayflick L, Moorehead P. The serial cultivation of human diploid strains. Exp Cell Res. 1961;25:585-621.

48.   Naylor RM, Baker DJ, van Deursen JM. Senescent cells: a novel therapeutic target for aging and age-related diseases. Clinical pharmacology and therapeutics. 2013;93:105-16.

49.   Zacarias-Fluck MF, Morancho B, Vicario R, Luque Garcia A, Escorihuela M, Villanueva J, et al. Effect of cellular senescence on the growth of HER2-positive breast cancers. J Natl Cancer Inst. 2015;107.

FIGURE LEGENDS

Figure 1. p53 induction increases BTK. (**A**) Western blot showing BTK and p53 expression in lysates of EJp53 in the absence of p53 (-) or 6 days after removal of tet to up-regulate p53 (+). (**B**) Western blot of lysates of HCT116 24 hours after being treated with 400μM of tert-Butyl Hydroxyperoxide (tBH) for 2 hours. (**C**) Western blot of lysates of HCT116 p53$^{+/+}$ and p53$^{-/-}$ treated with 1.5 μM doxorubicin for 20 hours. (**D**) Real time PCR showing changes in BTK mRNA expression in HCT116 cells treated with 1.5 μM doxorubicin for 20 hours. ** P=0.0016

(t-test). Results are the mean of three experiments. Error bars show standard deviation. (**E**) Kaplan-Meier survival curves of patients with CLL, breast or lung cancer, segregated according to high (red) or low (green) expression of BTK, obtained from public databases through a bioinformatics analysis using PPISURV (www.bioprofiling.de). Each graph represents a different GEO dataset (one CLL, one breast and two lung cancers).

Figure 2. BTK phosphorylates p53 and stabilizes its protein levels. (**A**) Western blot of EJp53 in the absence of p53 (-), 6 days after removal of tet to up-regulate p53 (+), or transfected with a plasmid containing BTK (+) or an empty vector control (-). Transfection was performed the 24 hours before tet removal and lysates were collected 2 days after transfection. (**B**) Real time PCR showing changes in p53 mRNA expression in HCT116 cells treated with 1.5μM doxorubicin for 20 hours, 24 hours after being transfected with an empty vector (Control) or a plasmid expressing BTK. Results show the mean of three experiments. Error bars show standard deviation. (**C**) Western blot showing BTK and p53 protein levels in lysates of EJp53 cultured in the absence of p53 (-) or 6 days after tet removal to induce p53 expression (+), treated with DMSO (-) or 0.5 μM Ibrutinib (+) from the beginning of the experiment, compared to EJp53 stably expressing a shRNA against BTK. (**D**) Western blot sowing p53 protein levels in lysates of EJp53 cultured in the presence or absence of tet to induce p53 for the specified time and treated with 0.5μM Ibrutinib or 2 μM CGI-1746 since the beginning of the experiment. (**E**) *In vitro* phosphorylation assay using recombinant BTK and GST-p53, either full length (FL) or fragments (comprising aminoacids 1-80, 100-300 or 300-393). (**F**) Western blot of lysates of the same cells in B, showing protein levels of BTK and Ser15 phosphorylated p53 (P-p53).

Figure 3. Increase of p53 activity in the presence of BTK. (**A**) Quantitative Real time PCR performed with RNA obtained from HCT116 transfected with an empty vector (Control) or BTK and treated with 1.5 µM doxorubicin for 20 hours. Data from two independent experiments. (**B**) Luciferase activity (in relative units) of a p21 or PUMA reporter transfected into the same cells as C. Data from three independent experiments. (**C**) ChIP performed in the same cells for the binding of p53 to the p21 and PUMA promoters. ** $P=0.0283$; * $P=0.0468$. For A-C: All statistics are unpaired t tests comparing doxorubicin treated samples with and without BTK, except when lines indicate otherwise. ns: $P > 0.05$; *: $P \leq 0.05$; ** $P \leq 0.01$; ***: $P \leq 0.001$; ****: $P \leq 0.0001$ (**D**) Western blot showing expression of BTK or a flag-tagged BTK missing its phosphorylation domain (ΔBTK) in HT1080 cells transfected with these plasmids or an empty vector (Control). (**E**) Luciferase activity (in relative units) of a p21 reporter transfected into the same cells as D in the presence or absence of 1.5 µM doxorubicin for 24 hours. Data from two independent experiments.

Figure 4. BTK contributes to p53-induced senescence. (**A**) Growth curves of EJp53 in the absence of p53 (Control) or after induction, treated with DMSO (Control and p53), 0.5 µM Ibrutinib (left plot) or 2 µM CGI-1746 (middle plot). Fresh media and drugs were added every time cells were counted. Right plot shows growth of EJp53 stable expressing a control shRNA (shLuci) or a specific one against BTK (shBTK) in the absence of p53 or after induction. Graphs represent mean of a triplicate experiment, error bars represent standard deviation. **** $P<0.0001$. (**B**) Left: EJp53 cells cultured in the presence of tet (Control) or 6 days after induction (p53), treated with DMSO (-) or 0.5 µM Ibrutinib (+) from the beginning of the experiment. Right: shLuci or shBTK EJp53 cultured in the same conditions. Magnification: 10x. (**C**) Colony

formation assay with the same cells, plus EJp53 treated with 2 μM CGI-1746 for 14 days. Graph representing mean percentage of colonies (compared to controls) of two independent experiments (each of them in duplicate). Error bars show standard deviation. Statistics of Control vs p53 cells: Ibrutinib, CGI and shBTK show no statistical significance (P=0.06, 0.125 and 0.05, respectively); Control and shLuci differences are significant (P<0.0001 and =0.01, respectively). (**D**) Growth curves of normal human diploid fibroblasts treated with DMSO (Control) or 0.3 μM Ibrutinib. Fresh media and drugs were added every time cells were counted. Graphs represent mean of a triplicate experiment, error bars represent standard deviation. (**E**) Representative Western blot showing expression of BTK, p16 and p53 in early (6 days) versus late (21 days) fibroblasts. (**F**) SA-β-gal staining of late passage fibroblasts (28 days) cultured in the presence of DMSO (Control) or Ibrutinib. Left: representative images. Right: quantitation of the same staining (graph show mean values of six different fields and error bars represent standard deviation).

Figure 5. Induction of the DNA damage and apoptotic pathways by BTK. (**A**) Western blot showing total BTK levels in lysates of HCT116 24 hours after being transfected with an empty vector (C) or a BTK vector (BTK). (**B**) Western blot of the same cells, showing levels of BTK, ATM and γH2AX. (**C**) Comet assay performed in HCT116 cells untreated (C), treated with 50μM H_2O_2 for 30 minutes on ice (a positive control of DNA damage), or 24 hours after being transfected with an empty vector (V) or a vector expressing BTK. 200 cells were scored for each condition. Error bars show SEM. **** P<0.0001 (unpaired t-test). (**D**) Representative FACS plots of HCT116 transfected with an empty vector (Control) or BTK (BTK), then stained with PI (top) or Annexin V (bottom). Numbers represent percentage of subG1 events (dead cells, top)

or Annexin V positive cells (apoptotic cells, bottom). (**E**) Western blot showing Caspase 3 (full length: 32 KDa; cleaved forms: 17 and 12 KDa) and PARP (full length: 116 KDa; top cleaved form: 89 KDa) cleavage in lysates of the same cells shown in A. (**F**) Left: Representative FACS analysis of PI-stained HCT116 treated with DMSO (Control), 1.5 µM doxorubicin or doxorubicin and 0.3 µM Ibrutinib for 48 hours. Numbers indicate the percentage of events in the SubG1 phase of the cell cycle (dead cells). Right: Plots showing percentage of events in the SubG1 in these cells. Results represent average of two independent experiments (done in triplicate or duplicate) and error bars show standard deviation. ** P=0.0092.
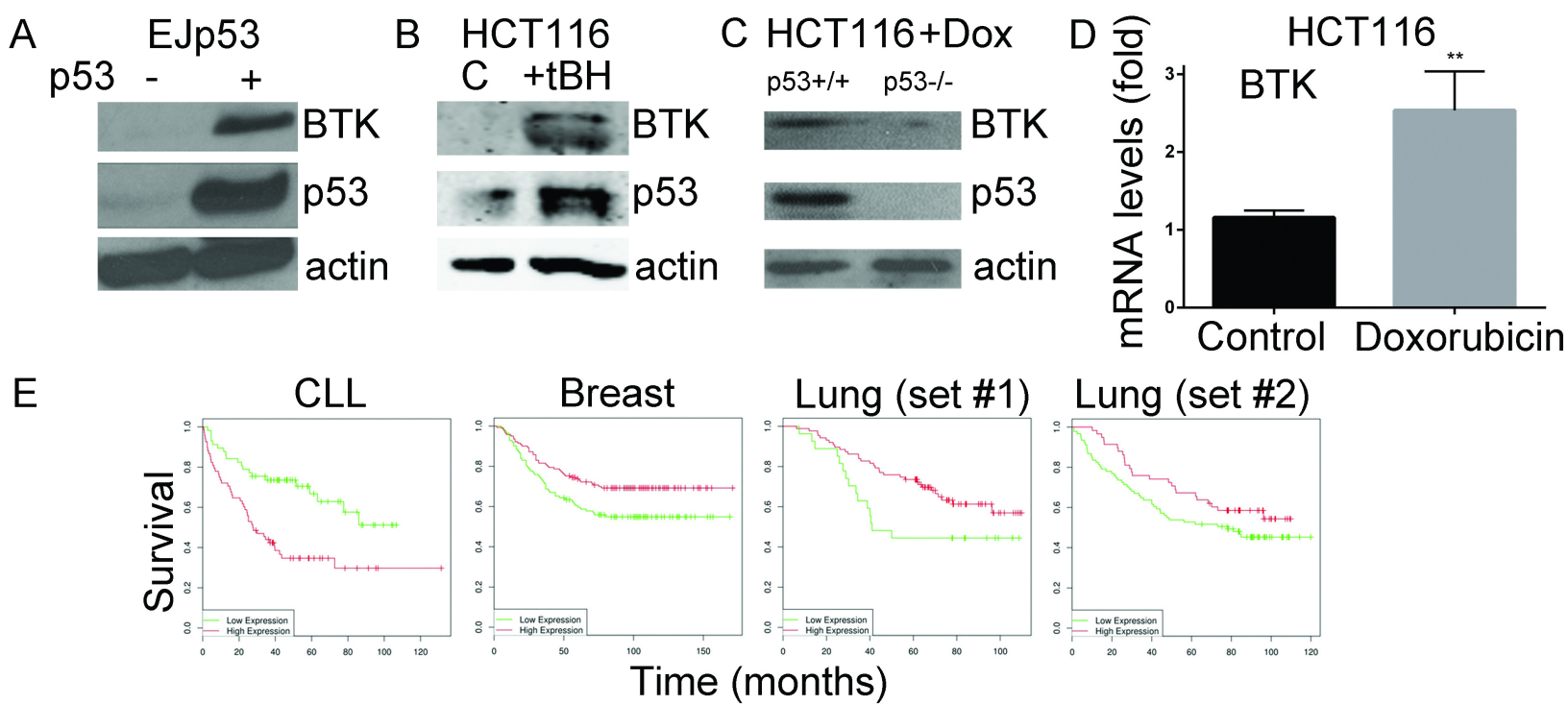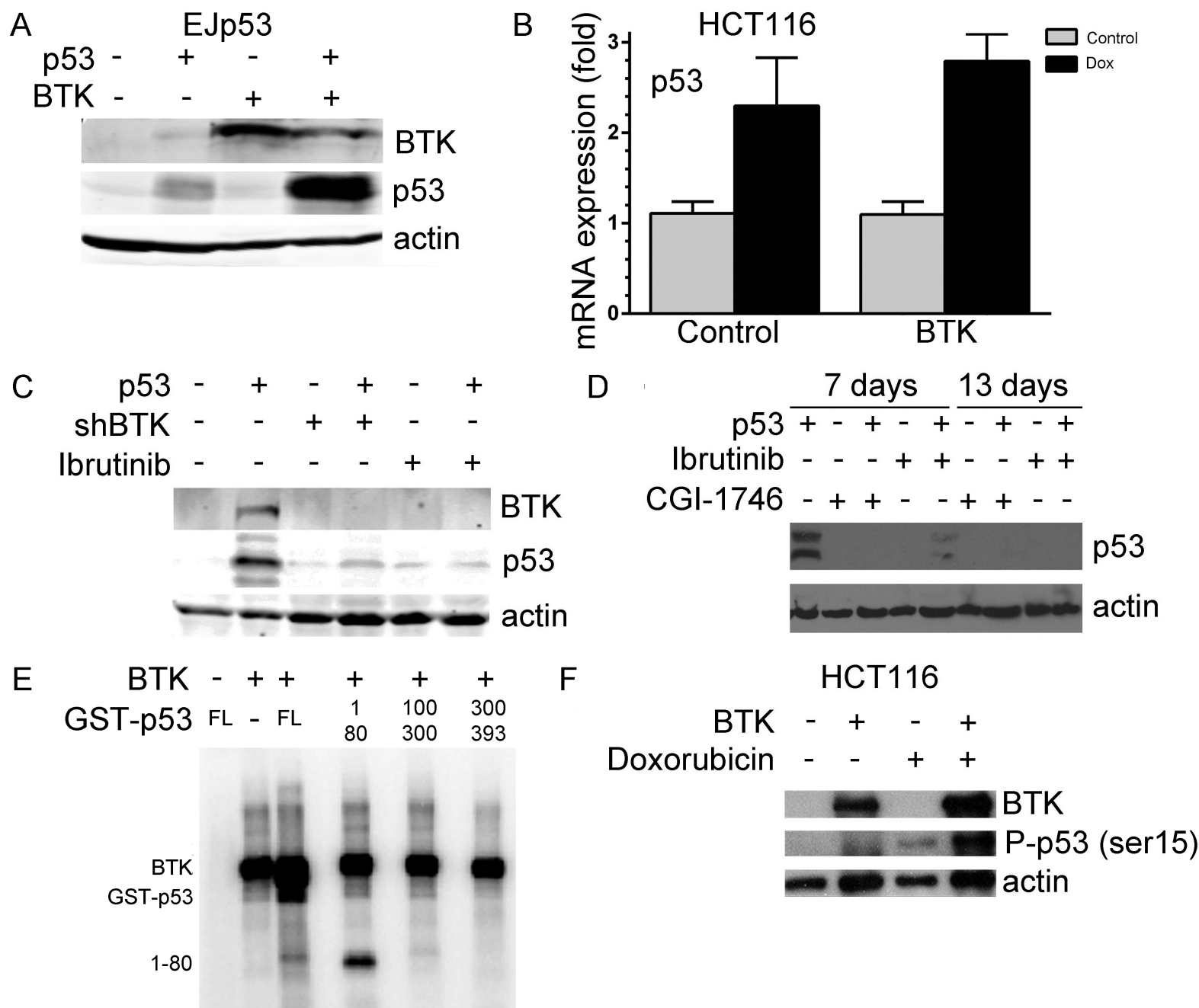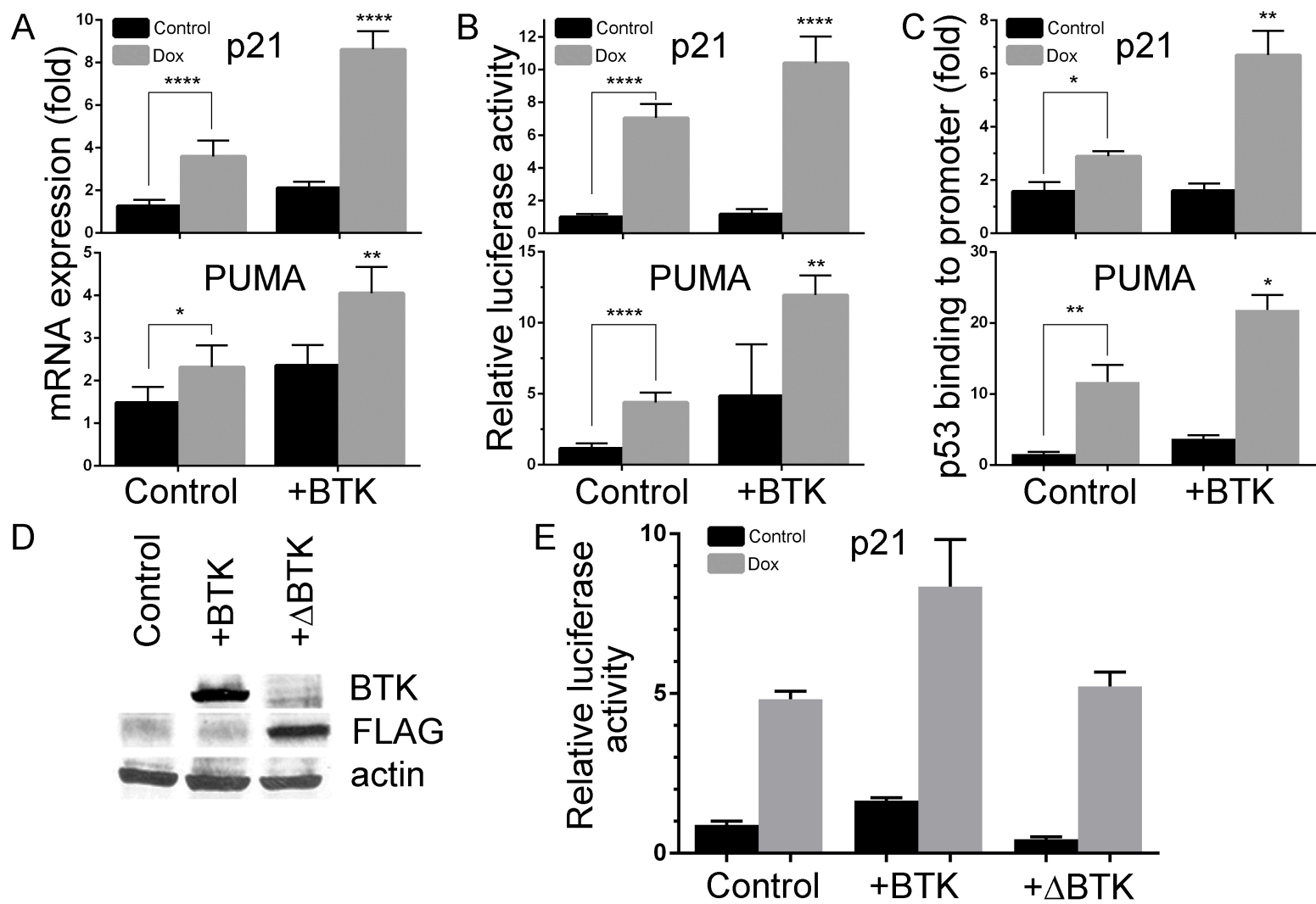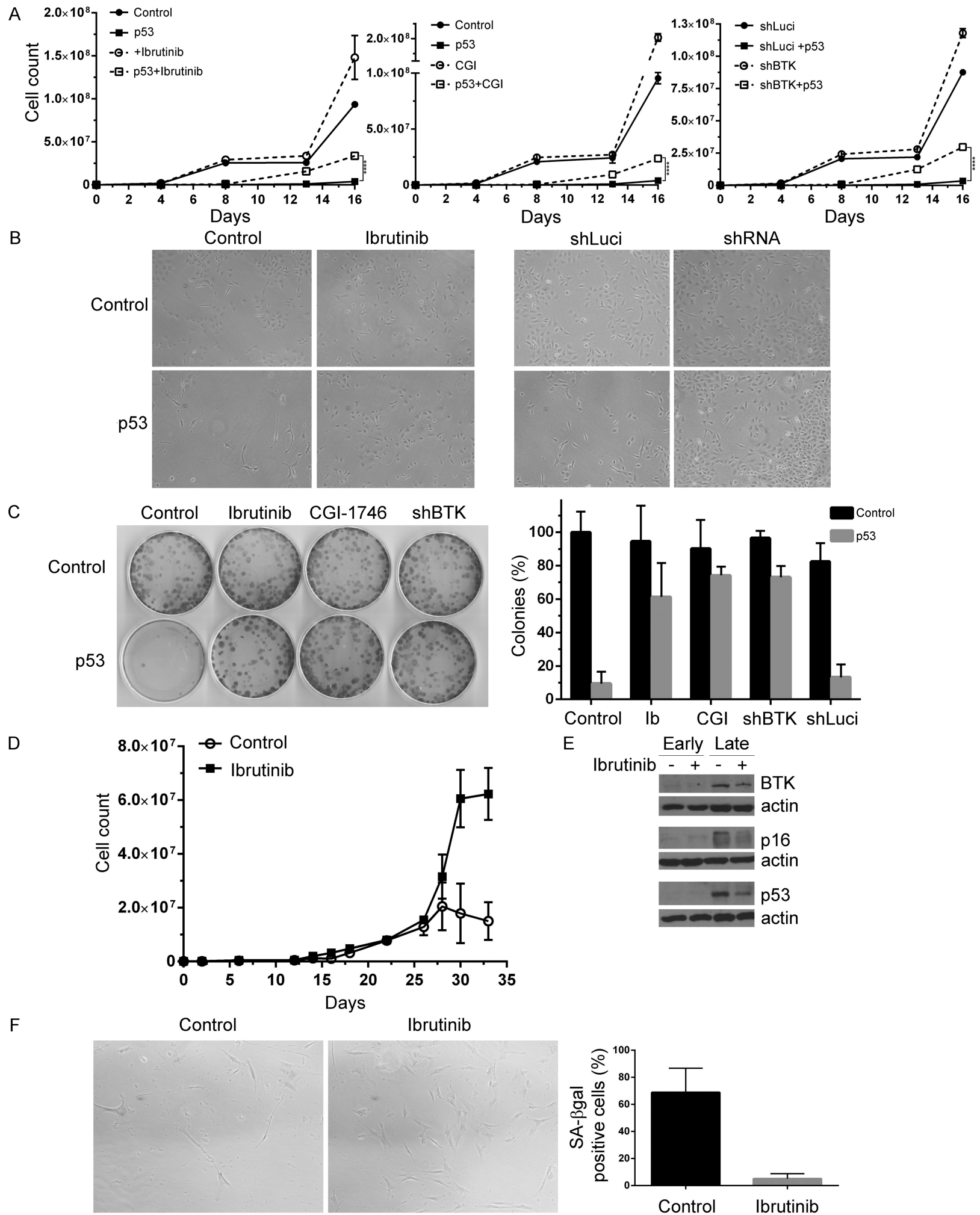
Figure 1

Figure 2

Figure 3

Figure 4

Figure 5